NENE
International Conference
Nuclear Energy for New Europe

Calculation of Neutron and Electron Transport in Self-Powered Neutron Detector for PWR Fuel Assembly

Jiří Závorka
University of West Bohemia
Univerzitní 26
30100 Plzeň, Czech Republic

ŠKODA JS a.s.
Orlík 266/15
32300 Plzeň, Czech Republic
zavorka@fel.zcu.cz

Martin Lovecký, Radek Škoda
University of West Bohemia
Univerzitní 26
30100 Plzeň, Czech Republic
lovecky@fel.zcu.cz, skodar@fel.zcu.cz

Czech Technical University in Prague,
Jugoslavskych partyzanu 1580/3,
160 00 Prague 6, Czech Republic

ABSTRACT

The research focused on a comprehensive study of calculating neutron and electron transport to evaluate Beta escape in a self-powered neutron detector (SPND) for a pressurized water reactor fuel assembly. The SPND is an important component used in nuclear power plants to monitor neutron flux in the core and indirect power distribution in the reactor core. Accurate neutron and electron transport calculations, considering the Beta escape phenomenon, are crucial for the proper functioning and performance assessment of the SPND.

This work presents a computational model based on the Monte Carlo method to simulate the transport of neutrons, and electrons, and determination the Beta escape process within the SPND. The model incorporates the PWR fuel assembly's geometry and material properties from the perspective of neutron transport and electron transport. The primary goal of this research is to improve the fundamental knowledge in determining beta escape, i.e., the probability of an electron reaching the collector in presented model SPND. It is an essential property that specifies the sensitivity of each of the detectors of this type. Moreover, it is basically crucial for in-core monitoring.

1 INTRODUCTION

The self-powered neutron detector (SPND) operates based on the (n,β) or (n,γ) reaction. The detector itself consists of two coaxial electrodes separated by insulation. These electrodes are connected to a cable with mineral insulation. In some cases, the cable also includes a compensation wire to offset the parasitic signal originating from the lead line. When placed in a radiation field, the inner electrode emits electrons, some of which have sufficient energy to penetrate the insulator. The emitter becomes positively charged, and the measured current corresponds to the radiation parameters of the field.

SPND offers several unique advantages. They do not require an external power supply, and their design is simple and robust. Their relatively compact dimensions make them suitable for in-core measurement, and they also prove good stability, especially under the influence of temperature and pressure. Additionally, they can produce a reproducible linear signal and have a relatively low burn-up rate, although this largely depends on the detector material.

Still, there are also certain disadvantages. They have a limited operational range, primarily because of their relatively low neutron sensitivity. Some emitters also require compensation for background noise, and certain emitters exhibit a delayed signal response. The casing material is typically corrosion-resistant steel or the nickel alloy Inconel, while the insulation is usually made from Al_2O_3, MgO, or SiO_2. Beta-emission SPDs have a delayed response. When placed in a neutron field, the emitter material becomes activated. These activated nuclei subsequently undergo beta decay. Some of the resulting electrons have enough energy to leave the emitter and pass through the insulator. The basic diagram is shown in Figure 1.

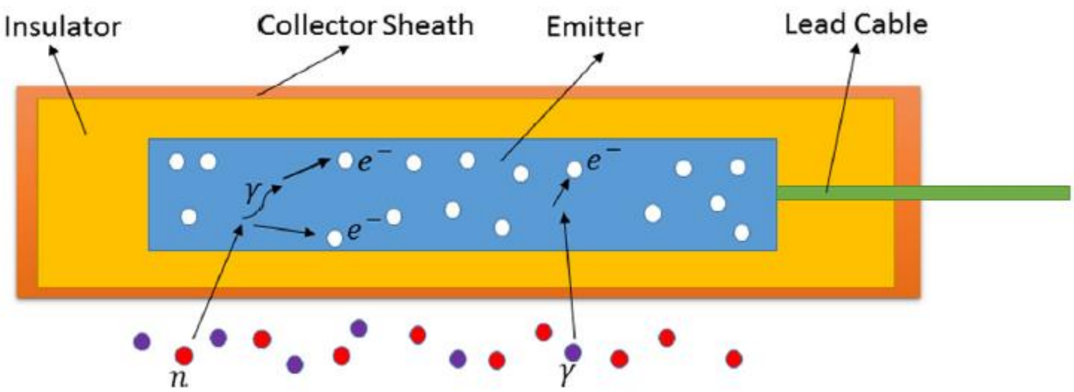

Figure 1: Schematic of self-powered neutron detector [1].

The process of electron transport from the emitter to the collector is complicated. It involves the interaction of electrons with atoms and their traversal through the potential barrier between the emitter and the collector. The probability that electrons will reach the collector is expressed by **β_{esc} (beta escape probability)**.

The primary research in this article mainly focuses on determining β_{esc} utilizing progressive computational approaches based on the Monte-Carlo method. Nevertheless, this study represents a preliminary evaluation of the self-powered neutron detector from the perspective of neutron transport and neutron transport calculation. The calculations do not include the resulting detected current, etc. The simulation is performed on a commonly used vanadium detector.

2 BETA ESCAPE PROBABILITY

Electrons and other charged particles fundamentally differ from neutrons and photon transport. Neutral particles interact infrequently, while electrons interact frequently due to the long-range Coulomb force. It is causing large number of short distance interactions. It is a very complex task, mainly when calculating the β_{esc} within the SPND. For this purpose, a Monte Carlo approach using the MCNP program with the latest electron data libraries [2].

2.1 Computation model

The parameters and geometry are based on the article published by Kyoon Ho, Cha in 2011 [4]. The details are in the following table:

Table 1: Material and specification of Vanadium SPND [4].

Part of SPND	Material	Density [g/cm^3]	Radius [cm]
Emitter	V-52	6.10	0.0565
Insulator	Al_2O_3	1.90	0.1015
Sheath	Inconel-600	8.44	0.1295

A Monte Carlo code, MCNP6, was used to simulate electron transport. The geometry was a simple 2D model based on the fundamental geometry presented in Table 1, and the emitter was divided into five sub-regions with preserving the same surface area. However, a challenging aspect of this calculation is using a reasonable source of electrons based on the radioactive date from the newest ENDF/b-VIII.0 library [7]. For analysis in this case, a continuous source for V-52 was used, as shown in Figure 2 [3].

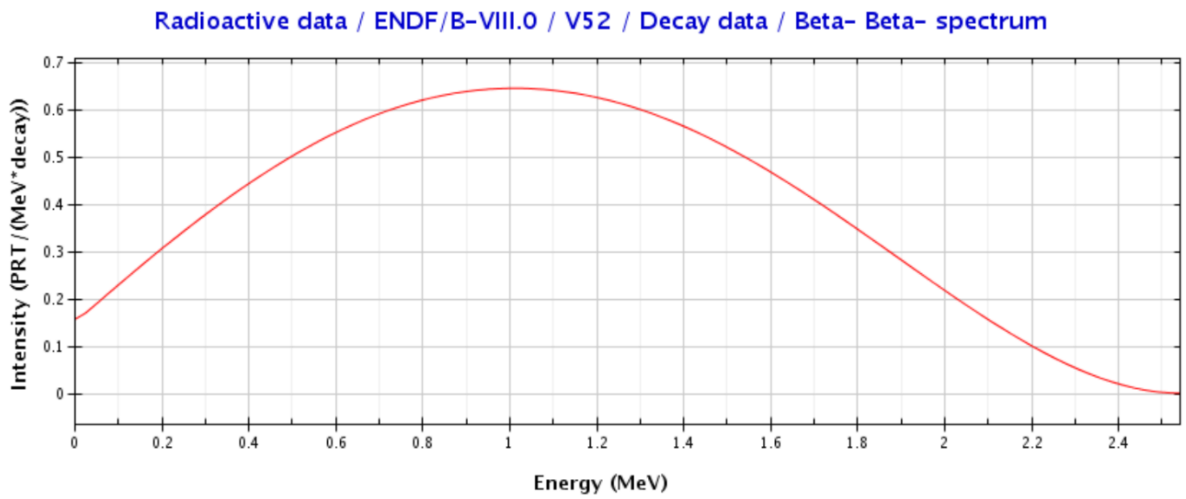

Figure 2: The β- spectrum for V-52 [3].

2.2 Comparison of results

Table 2: Result of β_{esc}.

This model	Kyoon Ho [4]	Warren [5]
0.53372	0.52778	0.56828 (Interpolated value)

2.3 Determination of β_{esc} for each concentric ring

As previously mentioned, the emitter is divided into five concentric rings (sub-division), each with an identical area. The following calculation presents the escape probability from each of these layers.

Table 3: Geometry of the emitter in the computation model.

Ring	1	2	3	4	5
Radius [cm]	0.0253	0.0358	0.0438	0.0506	0.0565

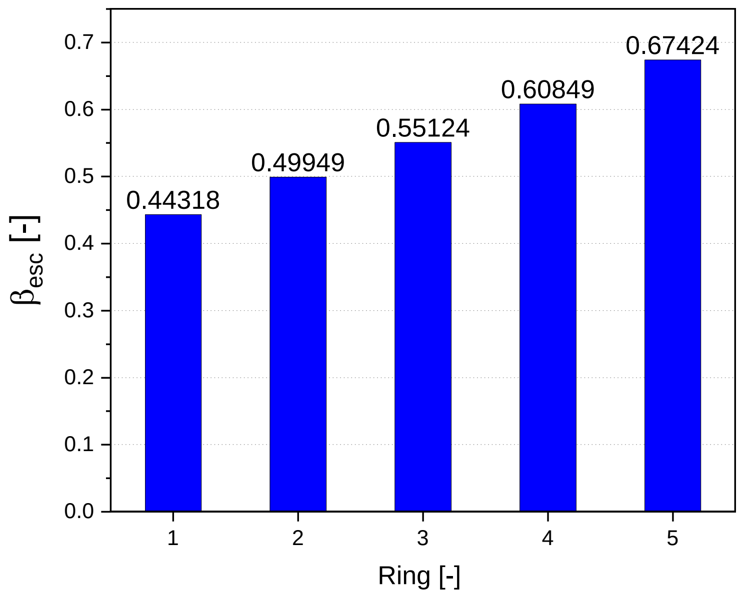

Figure 3: Determination of β_{esc} for concentric rings in the vanadium emitter.

As can be seen from the results in Figure 3, the calculations confirm that the probability of an electron reaching the collector increases if the electron is emitted near the edge of the emitter.

3 NEUTRON TRANSPORT

In the previous part was introduced the electron transport. Nevertheless, without the neutron interaction, there would be no electron production. This section presents a partial view of neutron transport on the example of the studied vanadium detector.

The beta decay scheme for the vanadium emitter is illustrated in Figure 4. The absorption reaction transforms V-51 into V-52, which subsequently emits an electron (β) with a half-life of 3.76 minutes. The primary equations presiding this chain are represented by Eqs. (1) and (2). A significant limitation of the V-SPND is its extended response time, attributed to V-52's considerable half-life — 99% of the signal exhibits a half-life of 3.76 minutes, while a mere 1% is prompt. The exceptionally low burn-up rate of V-SPND makes these detectors particularly significant for flux mapping in large-scale power reactors such as CANDU or PWR [1].

$$\frac{dV^{51}(t)}{dt} = -\varphi(t) \cdot \sigma_a^{51}.V^{51}(t), \tag{1}$$

$$\frac{dV^{52}(t)}{dt} = \varphi(t) \cdot \sigma_a^{51}.V^{51}(t) - \lambda_\beta^{V^{52}} V^{52}(t), \tag{2}$$

where

V^{51} : Atom density of vanadium-51
V^{52} : Atom density of vanadium-52
σ_a^{51} : Microscopic absorption cross section of V^{51}
$\lambda_\beta^{V^{52}}$: Beta decay constant of V^{52}

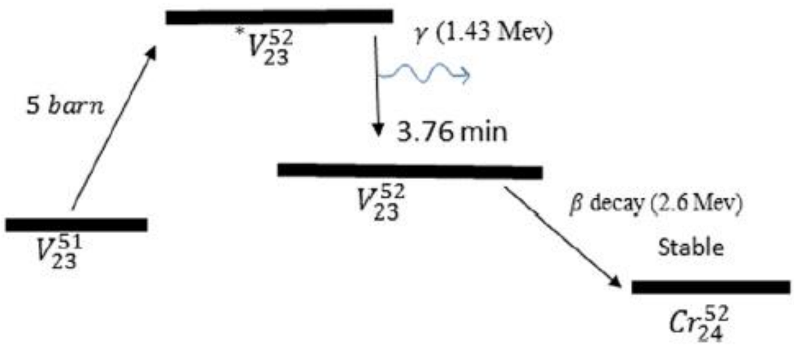

Figure 4: Decay chain of Vanadium [1].

3.1 Computation model

Neutron absorption in the emitter material is an essential characteristic for all SPNDs. The higher the neutron absorption cross-section, the better the detector sensitivity. However, the emitter material will degrade over time, and the content of the material will decrease (SPND burn-up). This characteristic can be very clearly characterized by the microscopic cross-section, see in Table 4 several examples of commonly used emitter materials.

Table 4: Microscopic cross sections for commonly used materials [8].

Isotope	**σ_a [barn]**
V-51	4.9
Rh-103	145.0
Ag-107	23.8
Co-59	37.0
Pt-195	24.0

For the appropriate monitoring of the power distribution in the core, it is necessary to know the accurate burn-out of the individual SPND, which is subsequently included in the SPND interpretation and subsequent reconstruction of the power distribution.

A simple demonstration of SPND burnup during reactor operation is performed in the following section. The neutronic calculations were done by Serpent transport code in version 2.1.32 [6] with the ENDF/B-VIII.0 continuous energy nuclear data library [7]. The SPNDs according to the geometry in Table 1 were placed in the APR1400 fuel assembly and burn up to 70,000 MWd/MTU. All parameters of the fuel assembly neutronic model are based on the report in [9].

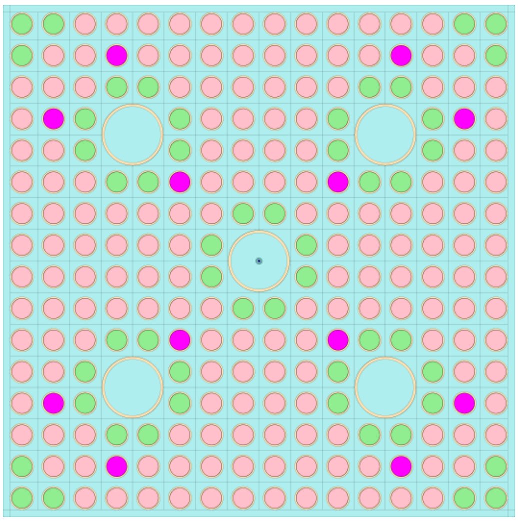

Figure 5: Model of fuel assembly with C1 radial profile with Vanadium SPND in central tube [9].

3.2 V-51 emitter during burn-up

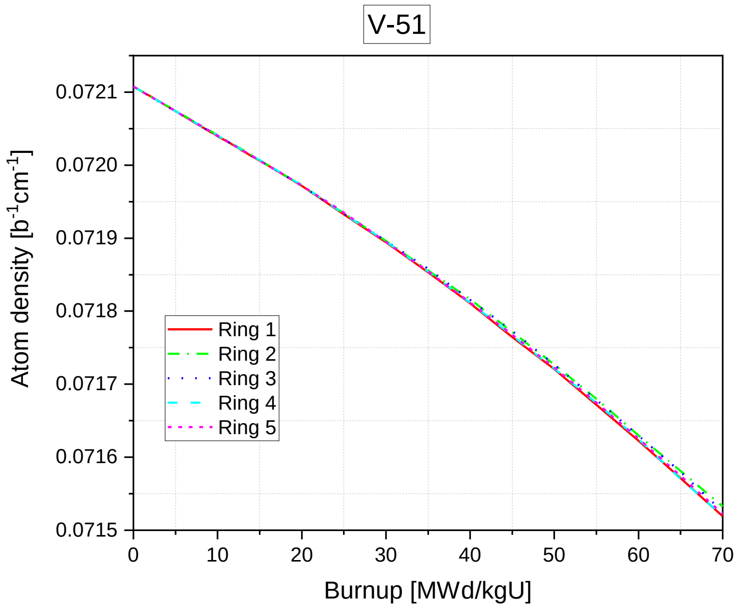

Figure 6: Results of atom density during burn-up process for individual rings of the vanadium emitter material.

4 CONCLUSIONS

In conclusion, this article comprehensively overviews the complex discipline of neutron and electron transport within self-powered neutron detectors (SPNDs). The first part of the paper focused on a general description of the SPND principle. It is followed by a more detailed verification of the Beta Escape Probability phenomena, specifically for the selected vanadium SPND representative. The β_{esc} was determined using a continuous V-52 electron source and Monte-Carlo approach. It was also compared to the study referenced in [4]. Furthermore, individual β_{esc} were evaluated for sub-divisions of the emitter model. It confirmed a dependency regarding the center of the emitter.

The second part of this research briefly ventured into neutron transport. Fundamental principles were explained, complemented by a basic burn-up calculation of SPNDs in fuel for the APR-1400 reactor type. This calculation shows a partial degradation of the emitter material during reactor operation.

This research provides a basic overview of the SPND and its context. Future work should focus on the neutron transport perspective (current interpretation) and the electron transport perspective.

ACKNOWLEDGMENTS

R&D has been funded by TN02000012 Centre of Advanced Nuclear Technology II (CANUT II) project.

REFERENCES

[1] F. Khoshahval, M. Park, H. Shin, P. Zhang, D. Lee, (2018). Vanadium, rhodium, silver and cobalt self-powered neutron detector calculations by Rast-K v2.0, Annals of Nuclear Energy, 111, 644–659., 2018, https://doi.org/10.1016/j.anucene.2017.09.048.

[2] J. Werner, S. Jeffrey, et al., MCNP Version 6.2 Release Notes, United States: N. p., 2018, Web, doi:10.2172/1419730.

[3] ENDF search, ENDF Search – JANIS, (n.d.), https://www.oecd-nea.org/janisweb/search/endf

[4] Kyoon Ho, Cha, Sensitivity Calculation of Vanadium Self-Powered Neutron Detector, Proceedings of the KNS spring meeting, (pp. 1CD-ROM), Korea, Republic of: KNS.

[5] H. D. Warren, Calculation Model for Self-Powered Neutron Detector, Nuclear Science and Engineering: 48. 331-342, 1972.

[6] J. Leppänen, M. Pusa, T. Viitanen, V. Valtavirta, T. Kaltiaisenaho, *The Serpent Monte Carlo code: Status, development and applications in 2013*, Annals of Nuclear Energy, 82, 2015.

[7] D. A., Brown, M. B., Chadwick, R., Capote, et al., ENDF/B-VIII.0: the 8th major release of the nuclear reaction data library with CIELO-project cross sections, new standards and thermal scattering data, Nuclear Data Sheets 148, 2018, 1-142, 10.1016/j.nds.2018.02.001.

[8] W. H. Todt, Characteristics of self-powered neutron detectors used in power reactors, Switzerland: European Nuclear Society, 1998.

[9] APR1400 Design Control Document Tier 2 (2018): Chapter 4 Reactor, APR1400-K-X-FS-14002-NO, Revision 3, (online).